New Phytologist

Research

Suberin deficiency and its effect on the transport physiology of young poplar roots

Paul Grünhofer[1], Ines Heimerich[1], Svenja Pohl[1], Marlene Oertel[1], Hongjun Meng[1], Lin Zi[1], Kevin Lucignano[1], Syed Nadeem Hussain Bokhari[2], Yayu Guo[3], Ruili Li[3], Jinxing Lin[3], Matthias Fladung[4], Tino Kreszies[5], Tyll Stöcker[6], Heiko Schoof[6] and Lukas Schreiber[1]

[1]Department of Ecophysiology, Institute of Cellular and Molecular Botany, University of Bonn, Kirschallee 1, 53115, Bonn, Germany; [2]Department Plant Biophysics and Biochemistry, Institute of Plant Molecular Biology, Czech Academy of Sciences, Biology Centre, Branišovská 31/1160, CZ-37005, České Budějovice, Czech Republic; [3]State Key Laboratory of Tree Genetics and Breeding, College of Biological Sciences and Technology, Beijing Forestry University, Beijing, 100083, China; [4]Thünen Institute of Forest Genetics, Sieker Landstraße 2, 22927, Grosshansdorf, Germany; [5]Department of Crop Sciences, Plant Nutrition and Crop Physiology, University of Göttingen, Carl-Sprengel-Weg 1, 37075, Göttingen, Germany; [6]Department of Crop Bioinformatics, Institute of Crop Science and Resource Conservation, University of Bonn, Katzenburgweg 2, 53115, Bonn, Germany

Author for correspondence:
Paul Grünhofer
Email: p.gruenhofer@uni-bonn.de

Received: *20 November 2023*
Accepted: *22 January 2024*

New Phytologist (2024) **242:** 137–153
doi: 10.1111/nph.19588

Key words: apoplastic barriers, Casparian bands, CRISPR, hydraulic conductivity, poplar adventitious root, suberin lamellae, transcriptomics, water and nutrient transport.

Summary

- The precise functions of suberized apoplastic barriers in root water and nutrient transport physiology have not fully been elucidated. While lots of research has been performed with mutants of *Arabidopsis*, little to no data are available for mutants of agricultural crop or tree species.
- By employing a combined set of physiological, histochemical, analytical, and transport physiological methods as well as RNA-sequencing, this study investigated the implications of remarkable CRISPR/Cas9-induced suberization defects in young roots of the economically important gray poplar.
- While barely affecting overall plant development, contrary to literature-based expectations significant root suberin reductions of up to 80–95% in four independent mutants were shown to not evidently affect the root hydraulic conductivity during non-stress conditions. In addition, subliminal iron deficiency symptoms and increased translocation of a photosynthesis inhibitor as well as NaCl highlight the involvement of suberin in nutrient transport physiology.
- The multifaceted nature of the root hydraulic conductivity does not allow drawing simplified conclusions such as that the suberin amount must always be correlated with the water transport properties of roots. However, the decreased masking of plasma membrane surface area could facilitate the uptake but also leakage of beneficial and harmful solutes.

Introduction

According to the composite transport model (CTM) of roots, three different radial transport pathways for water and solutes can be distinguished: the (1) symplastic; (2) apoplastic; and (3) transmembrane or transcellular pathway (Steudle *et al.*, 1993; Ranathunge *et al.*, 2017). In (1), water and solutes are taken up at the rhizodermis and travel radially through the plasmodesmata of the symplast into the xylem vessels. In (2), water and solutes remain in the porous apoplastic cell wall continuum until they reach the transport-limiting apoplastic barriers, Casparian bands (CB) and/or suberin lamellae (SL), of the endodermis, exodermis, or periderm, and are supposedly forced to enter the symplast to reach the xylem vessels. Whereas this has been shown numerous times for solutes, it has not clearly been proven experimentally for water. Finally, (3) resembles a combination of (1) and (2), and thus, frequent plasma membrane crossings of water and nutrients, for example, facilitated by the presence of aquaporins and transporters, are needed.

Longitudinal transport of water and solutes after arrival in xylem vessels does not represent a rate-limiting factor (Frensch & Steudle, 1989), but it can contribute to the passive leakage of water and solutes out of the xylem vessels (Chen *et al.*, 2019). This aspect can be significant and should not be neglected. Passive driving forces inducing root transport are composed of both water potential and solute concentration gradients. They are, in part, counterbalanced by active transmembrane solute transporters, but especially water flow will ultimately always follow the direction of the water potential gradient (Grünhofer & Schreiber, 2023). Therefore, the apoplastic barriers control the uptake and backflow of water and solutes into and out of the xylem vessels, respectively (Enstone *et al.*, 2003).

Suberin lamellae have historically been described as an apoplastic barrier conveying efficient ion diffusion resistance (Soukup & Tylová, 2018). Consequently, this was also generally concluded to be the case for the diffusion of water. Studies investigating, for example heavily suberized potato periderms, which

easily allow the exclusive study of water transport (Schreiber *et al.*, 2005a), seemed to confirm this conclusion. The transpiration barrier of potato periderms is as efficient as that of leaf cuticles, which perfectly limit non-stomatal water losses from the leaves to the atmosphere (Grünhofer *et al.*, 2022a). However, these water-transport-limiting properties of suberized tissues, including potato periderm, were essentially due to soluble lipids, often also called waxes, deposited in the suberin polymer and sealing it (Soliday *et al.*, 1979; Schreiber *et al.*, 2005a). Just recently, it was shown also for the atmosphere-exposed aerial roots of *Monstera deliciosa* that significant amounts of wax are deposited within the suberin polymer, and upon wax extraction, the transpiration increased up to 10-fold (Suresh *et al.*, 2022). In fact, this is the same with cuticles, which after wax extraction with only the structurally suberin-like cutin polymer remaining represent even two to three orders of magnitude weaker barriers for the diffusion of water (Schönherr & Lendzian, 1981). But similar amounts and compositions of lipids (waxes), which can be extracted from isolated suberized tissue obtained from strictly soil-grown roots, have not been described (Grünhofer & Schreiber, 2023).

Nevertheless, it has often been assumed without clear experimental evidence that increased amounts of root suberin must be correlated with decreased amounts of water transport (Taiz & Zeiger, 2002; Crang *et al.*, 2018; Nobel, 2020), and thus, suberin should always represent a primary barrier for the diffusion of water. But doubts about this simplified model have increased (Schreiber *et al.*, 1999, 2005b; Ranathunge *et al.*, 2011a; Kreszies *et al.*, 2018), and newer publications have re-emphasized the ion and solute barrier properties of root suberin (Barberon *et al.*, 2016; Chen *et al.*, 2019; Shukla & Barberon, 2021). While many corresponding studies focusing on root suberization were conducted with *Arabidopsis* or monocotyledonous crops, not much is known about tree species in general (Stoláriková *et al.*, 2012; Bagniewska-Zadworna *et al.*, 2014; Brunner *et al.*, 2015). The ion barrier effects of SL may indirectly be observed as shifts in the ionomes of leaves (Table 1), but they urgently need to be separated from those potentially originating from defects in CBs (Reyt *et al.*, 2021). And to which degree suberin also needs to be considered as a functional component of the lignin-based CBs, is still a matter of debate (Grünhofer & Schreiber, 2023). Taken together, CBs and SL do not exactly functionally replace each other, but, as has thoroughly been shown by studying the *enhanced suberin 1* (*esb1*) mutant of *Arabidopsis*, which is defective in CB formation but deposits ectopic amounts of suberin (Baxter *et al.*, 2009; Hosmani *et al.*, 2013; Pfister *et al.*, 2014), they may to some degree compensate for the defects in one another. This complex situation has been picked up by Calvo-Polanco *et al.* (2021), who introduced specific categories to summarize the defects prevalent in different *Arabidopsis* mutants: altered CB development, altered SL deposition, or a combination of both.

Based on this categorization, two especially important *Arabidopsis* mutants are exclusively altered in suberin biosynthesis without alterations of the CB development and function (Table 1). The genes knocked out by T-DNA insertion were *cyp86a1* (Höfer *et al.*, 2008) and *cyp86b1* (Compagnon *et al.*, 2009). Both proteins form the predominant suberin monomers, ω-hydroxy acids and α,ω-dicarboxylic acids (Vishwanath *et al.*, 2015; Rains *et al.*, 2017). Knock-out of these genes resulted in significantly reduced root suberin amounts in *cyp86a1* (category C=S-) and an altered composition without quantitative decreases in *cyp86b1* (category C=Sx; Calvo-Polanco *et al.*, 2021). In this study, the orthologous genes of *CYP86A1* and *CYP86B1* identified in *Arabidopsis* were simultaneously targeted in gray poplar (*Populus* × *canescens*) using a CRISPR/Cas9 double-knock-out transformation approach. It is of high scientific importance to eventually investigate the effects of decreased suberin contents in the roots of an economically important and perennial tree species as opposed to *Arabidopsis*, a short-lived annual plant. Our findings indicate that adventitious roots of gray poplar in their primary developmental stage can still regulate the uptake or leakage of water and nutrients even with a significantly impaired endodermal suberin barrier, or at least compensate for most of the effects caused.

Materials and Methods

Plant material and cultivation conditions

This study was conducted with the wild-type (WT) and transgenic lines (*CYP86A1* and/or *CYP86B1* knock-out by CRISPR/-Cas9) of *P.* × *canescens* (Aiton) Sm. clone INRA 717-1B4 (*P. tremula* × *P. alba*; Leplé *et al.*, 1992). Plant cultivation (tissue culture, soil, and hydroponics) and experiment preparation were carried out in a climate chamber under long-day (16 h : 8 h, illumination : darkness) conditions. All investigated plants were propagated in axenic tissue culture and transplanted into soil after 6–8 wk of growth. The cultivation in soil was continued for another 8–10 wk. At a total plant age of 14–18 wk, the soil-grown plants were dissected into stem cuttings and transferred into hydroponic setups to facilitate the formation of adventitious roots (for details, see Grünhofer *et al.*, 2021). Hydroponic cultivation was mostly carried out for 5 wk, and for 7 wk in some additional experiments (see 'Prolonged period of cultivation' in the Materials and Methods section). Further details about the cultivation conditions can be found in Supporting Information Methods S1. About six independent batches of plants (each batch comprising four to six clones per line) were transplanted into soil and consequently transferred into hydroponics throughout the year. At least three repetitions of each experiment were performed temporally separated, and thus, the data of each experiment rely on independent biological (clones), as well as seasonal (batches) replicates of $n \geq 3$. Details about the exact sample size used in each experiment are provided in the figure legends.

Generation of transgenic poplar lines

The *P.* × *canescens* clone INRA 717-1B4, with its genome completely sequenced (Mader *et al.*, 2016), is especially well-suited for *Agrobacterium*-mediated transformation (Leplé *et al.*, 1992). In a CRISPR/Cas9 double-knock-out approach (the targeted

Table 1 Shifts in leaf ionomes of *Arabidopsis* mutants as a consequence of alterations in the apoplastic barriers Casparian bands and/or suberin lamellae.

Category[1]	Targeted gene[2]	Reference	Li	B	Na	Mg	P	S	K	Ca	Mn	Fe	Co	Ni	Cu	Zn	As	Se	Rb	Sr	Mo	Cd	Cs
C-S+	*ESB1*	Baxter *et al*. (2009)	=	=	+	−	=	+	+	−	−	−	=	=	=	−	+	+	na	na	+	=	na
C-S+	*ESB1*	Hosmani *et al*. (2013)	−	=	−	−	=	+	+	−	−	−	=	=	=	=	=	−	+	−	+	=	na
C-S+	*ESB1*	Calvo-Polanco *et al*. (2021)	na	na	=	=	=	na	+	−	=	=	na	na	=	=	na	na	na	na	na	na	na
C-S+	*CASP1 CASP3*	Hosmani *et al*. (2013)	−	=	+	−	=	+	+	−	−	−	=	=	+	=	=	−	+	−	+	=	na
C-S+	*MYB36*	Calvo-Polanco *et al*. (2021)	na	na	=	+	=	na	+	−	=	=	na	na	=	=	na	na	na	na	na	na	na
C-S+	*MYB36*	Kamiya *et al*. (2015)	+	−	+	+	=	=	+	−	−	−	−	−	+	+	=	=	+	−	+	+	na
C-S+	*MYB36*	Reyt *et al*. (2021)[3]	~+	~=	~+	~+	~+	~+	−	~=	−=+	~=	~=	~+	~=	=	−=+	~=	−	~+	~+	~=	na
C-S+	*MYB41*	Shukla *et al*. (2021)	+	−	−	−	−	=	−	−	+	−	+	=	=	+	=	na	−	−	+	−	na
C-S+	*LCS2*	Li *et al*. (2017)	=	+	+	=	=	+	+	−	−	−	+	=	+	=	+	=	+	−	+	+	na
C-S=	*SGN3*	Pfister *et al*. (2014)[3]	na	=	~=	+	~ =	na	−	~=	~=	~=	~=	na	~=	~−	na	na	na	~=	~=	na	+
C-S=	*SGN3*	Calvo-Polanco *et al*. (2021)	na	na	=	+	=	na	−	=	=	=	na	na	=	−	na	na	na	na	na	na	na
C-S=	*SGN3*	Reyt *et al*. (2021)[3]	~+	~=	~+	~+	~=	~+	−	=	~=	=	=	~=	−=+	=	~=	~=	−	~=	~=	~−	na
C-S=	*SGN3 ESB1*	Calvo-Polanco *et al*. (2021)	na	na	+	+	=	na	−	=	=	+	na	na	=	−	na	na	na	na	na	na	na
C-S=	*SGN3 MYB36*	Reyt *et al*. (2021)[3]	+	~+	+	~+	−=+	+	−	~=	−=+	−=+	~−	~+	−=+	~−	+	=	−	~+	~=	~−	na
C=S+	*MYB41*	Shukla *et al*. (2021)	+	−	−	−	−	−	−	−	=	−	−	+	+	+	−	na	−	−	+	+	na
C=S+	*GELP51*	Calvo-Polanco *et al*. (2021)	na	na	=	=	=	na	=	=	=	=	na	na	=	=	na	na	na	na	na	na	na
C=S+	*ANAC038*	Calvo-Polanco *et al*. (2021)	na	na	=	=	=	na	=	=	=	=	na	na	=	=	na	na	na	na	na	na	na
C=Sx	*CYP86B1*	Compagnon *et al*. (2009)	na	na	=	=	=	na	=	=	na	na	na	na	na	na	na	na	na	na	na	na	na
C=Sx	*CYP86B1*	Calvo-Polanco *et al*. (2021)	na	na	=	=	=	na	=	=	=	=	na	na	=	=	na	na	na	na	na	na	na
C=S-	*CYP86A1*	Calvo-Polanco *et al*. (2021)	na	na	=	=	=	na	=	=	=	=	na	na	=	=	na	na	na	na	na	na	na
C=S-	*CYP86A1 CYP86B1*	Calvo-Polanco *et al*. (2021)	na	na	=	=	=	na	=	=	=	=	na	na	=	=	na	na	na	na	na	na	na
C=S-	*CDEF*	Barberon *et al*. (2016)[3]	+	~=	~+	~+	~=	~=	~−	~=	~=	~=	~=	~=	~=	~=	~+	~+	~−	=	~=	~=	=
C=S-	*CDEF*	Shukla *et al*. (2021)	+	+	+	+	−	=	−	+	+	−	=	−	+	−	+	na	−	+	+	−	na
C=S-	*MYB41 MYB53 MYB92 MYB93*	Shukla *et al*. (2021)	+	+	+	=	−	−	=	+	+	=	=	−	−	=	+	na	=	=	−	=	na
C?S-	*GPAT5*	Compagnon *et al*. (2009)	na	na	=	−	=	na	−	−	na	na	na	na	na	na	na	na	na	na	na	na	na

C-S+, defective Casparian bands and increased suberin contents; C-S=, defective Casparian bands and equal suberin contents; C=Sx, functional Casparian bands and equal suberin contents but with altered composition; C=S-, functional Casparian bands and decreased suberin contents; C?S-, functionality of Casparian bands not investigated and decreased suberin contents; C=S+, functional Casparian bands and increased suberin contents. Red/+, significantly increased; blue/−, significantly reduced; gray/=, no change; purple/−=+, all three types of changes were observed; ~, observed in most cases if several analyses were performed; na, not available; significance was tested at $P < 0.05$ or $P < 0.01$.

[1]Categories according to Calvo-Polanco *et al*. (2021), nomenclature simplified and carried over to further publications.

[2]The listed genes were targeted with various knock-out or over-expression approaches using differently designed constructs, for details the reader is advised to the original article.

[3]Also different growth conditions or samples originating from different laboratories were evaluated.

genes were the poplar orthologs of *CYP86A1*, AT5G58860, and *CYP86B1*, AT5G08250, described in *Arabidopsis*), a leaf disk transformation was performed (Fladung *et al.*, 1997). Due to the known whole-genome duplication, a set of four orthologous gene targets were selected based on the genome of *P. trichocarpa* (Tuskan *et al.*, 2006): *CYP86A1_1*, Potri.009G043700; *CYP86A1_2*, Potri.001G249700; *CYP86B1_1*, Potri.007G072100; *CYP86B1_2*, Potri.005G092200. Since *P.* × *canescens*, as a hybrid, has two alleles per *P. trichocarpa* ortholog, this resulted in up to eight potential gene targets (Grünhofer *et al.*, 2022b; Fig. S1). The transformation vector (Notes S1) containing guide-RNA for two target sites (T1, T2) per gene *CYP86A1* and *CYP86B1* (Fig. S1) as well as an *hptII* resistance cassette for subsequent Hygromycin selection were introduced into the leaf tissue. Further details about this transformation procedure, the analytical mutant screening for root suberin amount and composition, and the target gene editing analysis by sequencing (Notes S2) are provided in Fig. S2.

Plant development

At harvest, the plants were subjected to various physiological measurements to characterize and compare their developmental stage after 5 wk of cultivation in hydroponics. The stomatal conductance (LI-600 Leaf Porometer; Li-Cor, Lincoln, NE, USA) and the chlorophyll content of leaves (Force A device; Dualex Scientific, Orsay, France) were measured non-invasively with intact plants. For the determination of the root and shoot lengths (measured with a ruler), as well as the osmotic potentials (freezing point osmometer, OSMOMAT 030; Gonotec, Berlin, Germany) and relative water contents (RWC) of shoots and roots, and the investigation of the leaf ionome (ICP-OES, Vista-RL Simultaneous ICP-OES; Varian Inc., Palo Alto, CA, USA), the plant organs had to be harvested. The osmotic potentials of the supernatants were calculated after milling (Retsch MM400; Retsch GmbH, Haan, Germany) and centrifugation of the sample following the Van't Hoff equation ($\Psi_s = -R\,T\,i\,C$, in which R – universal gas constant, T – absolute temperature, i – Van't Hoff factor, and C – osmolarity of the supernatant). The RWC was calculated based on relating fresh weight (FW) and dry weight (DW) after drying the samples for 24 h at 60°C following RWC = (FW-DW) FW^{-1}. The mineral concentrations were measured with 100 mg of oven-dried and powdered leaf material after digestion in 4 ml of concentrated HNO_3 and 2 ml of 30% H_2O_2 at 200°C and 15 bar for 75 min.

Casparian band and suberin lamellae development

The development of CBs was histochemically surveilled using 0.1% (w/v) berberine hemi-sulfate and 0.5% (w/v) aniline blue (Brundrett *et al.*, 1988). The formation of SL was investigated by 0.01% (w/v) fluorol yellow 088 staining (Brundrett *et al.*, 1991). At least six adventitious roots of average length (±3 cm of the calculated mean) of each mutant were selected and stained with either berberine–aniline or fluorol yellow 088. The roots were divided into 10% increments (where 0% represents the root tip and 100% the root base), and selected segments were investigated by epifluorescence microscopy. Further details about the histochemical analysis can be found in Methods S1. Following previous studies focusing on the root development of the *P.* × *canescens* clone 84K (Grünhofer *et al.*, 2021, 2022b, 2023), two functional developmental zones important for the chemical suberin analysis could also be identified with 5-wk-old roots of INRA 717-1B4. Zone A, defined by no observable endodermal suberization in the WT, ranged from 0% to 21.5% relative root length, and Zone B, characterized by patchy endodermal suberization, constituted the remaining 21.5–100%. By contrast, more mature roots of 7 wk of age (see 'Prolonged period of cultivation' in the Materials and Methods section) exhibited root zones of no suberization (Zone A, 0–20%), patchy suberization (Zone B, 20–50%), full suberization (Zone C, 50–70%), and periderm development (Zone D, 70–100%).

Root suberin composition and amount

Between 10 and 20 individual roots were pooled to form one biological replicate after removing lateral roots and separating the main root into the functional zones (5-wk-old: A: 0–21.5%; B: 21.5–100%; 7-wk-old: A: 0–20%, B: 20–50%, C: 50–70%, D: 70–100%) using a razor blade. The samples were then further prepared for analytical analysis following the protocol described in Baales *et al.* (2021). Further details about the chemical analysis can be found in Methods S1. The acquired suberin amounts were finally related to the endodermal surface area (A_{en}) of each zone since no formation of an exodermis has been observed. Here, the root zones were treated as truncated cones due to their secondary thickening in diameter (Grünhofer *et al.*, 2021).

Transport of water and solutes

For more detailed descriptions of root pressure probe (Steudle *et al.*, 1987) and pressure chamber experiments (Miyamoto *et al.*, 2001) performed especially with rooted stem cuttings of poplars, the reader is advised to Grünhofer *et al.* (2021). Both methods are in accordance with the CTM (Steudle *et al.*, 1993; Ranathunge *et al.*, 2017) and were used to evaluate the conductivity of roots toward water and solutes.

In pressure probe experiments, whole individual adventitious 5-wk-old roots were mounted to the root pressure probe. The fixed root was subjected to either osmotic or hydrostatic pressure changes. The induced changes in root pressure then allowed the calculation of the reflection coefficient σ_{sr}, as well as the osmotic hydraulic conductivity Lp_r(OS) and the hydrostatic hydraulic conductivity Lp_r(HY) in m s^{-1} MPa^{-1}.

In pressure chamber experiments, stem cuttings with 5- and 7-wk-old whole root systems were fixed in the device, and manipulation of the applied pneumatic pressure from 0 to 0.4 MPa in 0.1 MPa increments resulted in different amounts of xylem sap exuding from the trimmed shoot. The collection of xylem sap at each pressure interval also allowed the calculation of the osmotic (at 0 MPa) hydraulic conductivity Lp_r(OS) and the hydrostatic (at 0.1–0.4 MPa) hydraulic conductivity Lp_r(HY) in m s^{-1} MPa^{-1}.

A modification of this method is the addition of defined amounts of solutes to the root medium (in this case, only water)

inside the pressure chamber and measuring the bypass flow of the given chemicals through the root into the shoot tissue at constant pneumatic pressures. In this study, the fluorescent apoplastic tracer dye PTS (trisodium, 3-hydroxy-5,8,10-pyrenetrisulfonate; Hanson *et al.*, 1985) and the osmotically active sodium chloride (NaCl; Wang *et al.*, 2019) were used. The PTS and NaCl bypass flow in % was calculated by relating the xylem exudate concentrations to the applied concentrations in the root medium. Further details about the bypass flow analysis can be found in Methods S1.

To further assess the solute uptake dynamics of intact plants, stem cuttings comprising well-developed shoots and root systems (characterized in Fig. 1) were exposed the photosynthesis inhibitor Metribuzin (Bayer, Leverkusen, Germany) in the nutrient solution. The impact of this herbicide on the photosynthetic machinery, once taken up by the roots and translocated into the leaves, was quantified using pulse amplitude modulated (PAM) chlorophyll fluorometry (Junior-PAM, Walz, Effeltrich, Germany). By relating the pre-treatment photosynthetic yield (in healthy plants, usually *c.* 70%) to the declining post-treatment photosynthetic yield, 50% (yield below *c.* 35%) and 95% (yield below *c.* 3.5%) yield inhibition times ($t_{50\%}$ and $t_{95\%}$, respectively) were calculated. Further details about the photochemical analysis can be found in Methods S1.

Transcriptomic changes

Based on the observation of root suberin deposition, root segments of 20–50% relative distance that comprised the onset of SL development in the WT were harvested. To form one biological replicate, six roots were pooled and RNA isolation was performed with the *Quick*-RNA Miniprep Kit following the manufacturer's instructions (Zymo Research, Freiburg, Germany). Sequencing was carried out on a NovaSeq 6000 system (NGS Core Facility, University Hospital of Bonn, Germany) using a Lexogen QuantSeq 3′-mRNA protocol. The raw sequencing data have been deposited at the sequence read archive (SRA), PRJNA940679. The reads were aligned against a genome index of the reference sequence and annotation of *P.* × *canescens* genotype 84K (Qiu *et al.*, 2019). Differentially expressed features between WT and the four mutants were identified with the package EDGER v.3.26.4 (Robinson *et al.*, 2010) using the R programming language (R Core Team, 2023). Only features passing a false discovery rate (FDR) threshold of < 0.05 (Benjamini–Hochberg) were considered as differentially expressed genes (DEGs). Further details about and results of the RNA-sequencing analysis can be found in Methods S1 and Notes S3, respectively. Phylogenetic analyses and functional annotations were based on the results reported by Grünhofer *et al.* (2022b).

Reverse transcription quantitative polymerase chain reaction (Methods S1; Notes S2) additionally confirmed selected outstanding genes of this RNA-sequencing analysis (Table 2) with independently cultivated sets of plants.

Prolonged period of cultivation

In addition to 5 wk of cultivation in hydroponics, selected experiments were repeated with a 7-wk-long hydroponic cultivation using just the WT and mutant line (*cyp86a1_1,2;b1_1*). This most affected mutant line was selected based on time and material constraints, as it promised to deliver the most outstanding results. A prolonged cultivation period was intended to facilitate a higher degree of individual root and root system maturation. This included the development of a full endodermal suberization as well as periderm formation, because both processes significantly reduce the prevalence of non-suberized passage cells and should thus further emphasize the physiological effects of significant mutation-induced root suberin deficiencies.

Statistical analysis

The statistical analysis of the overall sample size (based on at least three independent biological and seasonal replicates) provided in the figure legends and figure preparation were carried out with OriginPro 21b (OriginLab Corp., Northampton, MA, USA). The normality of data was assessed with the Shapiro–Wilk test. Means of normally distributed data were then compared with a one-way ANOVA with Fisher's LSD *post hoc* test, and data were presented using means with standard deviations or boxplots. By contrast, sets of not normally distributed data were compared with a Kruskal–Wallis ANOVA and visualized using only boxplots. Except for experiments involving the root pressure probe and pressure chamber, whose results were evaluated at $P < 0.01$ due to their often-reported high variability (Steudle & Meshcheryakov, 1996; Zimmermann *et al.*, 2000; Miyamoto *et al.*, 2001; Ranathunge *et al.*, 2011a; Kreszies *et al.*, 2019), all other tests were carried out at $P < 0.05$. Statistically significant differences are indicated by differential letters.

Results

Generation of transgenic poplar lines

A set of eight promising putatively transformed lines (the presence of *cas9* and/or *hptII* was checked by PCR) was included in a chemical analytical screening to check for differences in the root suberin amount and composition (Fig. S2). The phenotypically remarkable lines were additionally included in a genetic screening performed by DNA sequencing (Fig. S2). The four mutant lines chosen to be analyzed in further experiments were either edited in three out of four alleles of *CYP86A1_1* and *CYP86A1_2* and both alleles of *CYP86B1_1* (mutant *cyp86a1_1,2;b1_1*), one out of two alleles of *CYP86A1_2* and both alleles of *CYP86B1_1* (mutant *cyp86a1_2;b1_1*), both alleles of *CYP86A1_1* and both alleles of *CYP86B1_1* (mutant *cyp86a1_1;b1_1*), or in all four alleles of only *CYP86A1_1* and *CYP86A1_2* (mutant *cyp86a1_1,2*).

Plant development

The development of the 14- to 18-wk-old soil-grown mutant plants used to initiate a hydroponic experiment and the poplar mutants cultivated in hydroponics was highly similar to that of the WT. After 5-wk-long hydroponic cultivation, neither root nor shoot lengths (Fig. 1a), nor the osmotic potentials of roots or leaves (Fig. 1b), deviated considerably from those of the WT.

New Phytologist

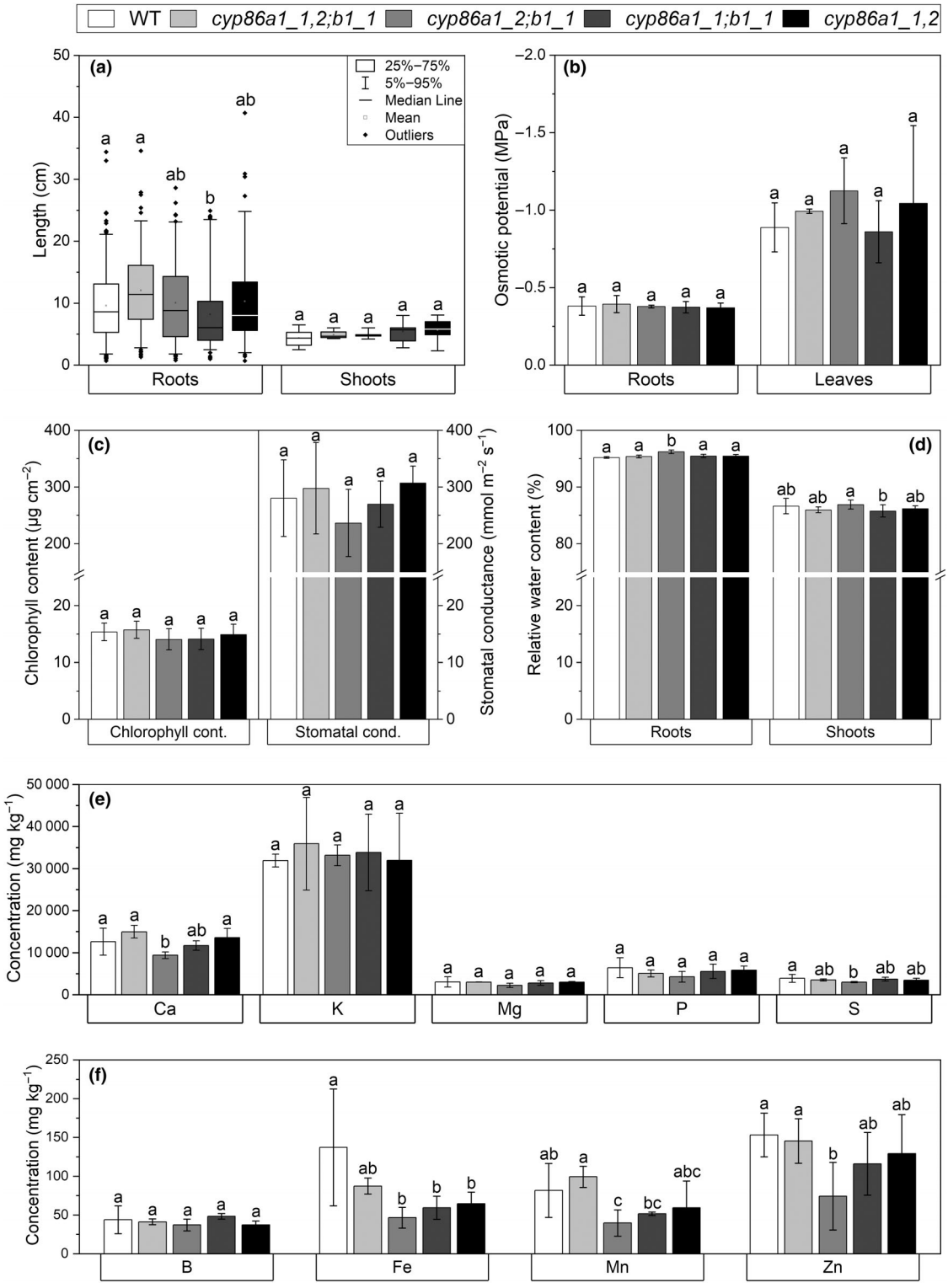

Fig. 1 Physiological parameters of the *Populus* × *canescens* wild-type (WT) and four suberin mutants after 5 wk of cultivation in hydroponics. Root and shoot length (a), osmotic potentials of roots and leaves (b), chlorophyll content and stomatal conductance of leaves (c), relative water content of roots and shoots (d), and macro- (e) and micronutrient (f) composition of leaves are compared. Boxplots or means with SD (n = 85–218 roots and 4–10 shoots (a), 4–13 (b–d), 3–4 (e, f)) are shown, and differential letters indicate significant (Kruskal–Wallis ANOVA (a) and one-way ANOVA with Fisher's LSD *post hoc* test (b–f)) differences at $P < 0.05$. The boxplots designate: box = 25–75%, whisker = 5–95%, horizontal line = median, empty square = mean, filled diamond = outlier.

Table 2 Differential root expression analysis of the *Populus* × *canescens* wild-type and four suberin mutants after 5 wk of cultivation in hydroponics.

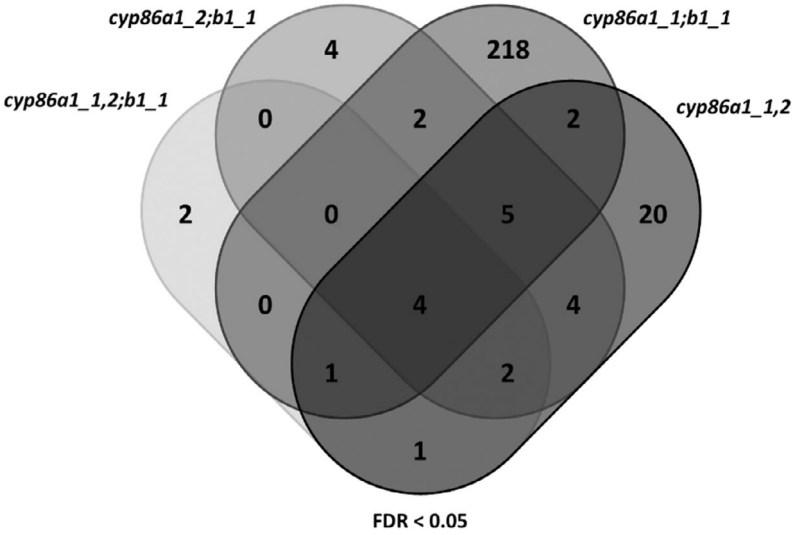

A. thaliana Gene name	Description	*P.* × *canescens* Gene ID	Log_2FC *cyp86a1_1,2; b1_1*	Log_2FC *cyp86a1_2; b1_1*	Log_2FC *cyp86a1_1; b1_1*	Log_2FC *cyp86a1_1,2*	Function
DEGs in 4 out of 4 mutants							
S8H	Scopoletin 8-hydroxylase	Pop_A05G073329	+10.8	+11.8	+9.5	+13.1	Involved in biosynthesis of coumarins (e.g. scopoletin), which mobilize Fe previously bound to negatively charged cell wall
FRO2	Ferric reduction oxidase 2	Pop_A14G044793	+9.7	+11.2	+9.3	+12.0	Reduction of Fe^{3+} to Fe^{2+}, to facilitate the uptake from root medium into plant tissue
IRT1	Fe(2+) transport protein 1	Pop_G15G010604	+11.1	+13.0	+11.0	+13.6	Mediates the uptake of a variety of divalent cations including Fe^{2+}
IRT1	Fe(2+) transport protein 1	Pop_A15G084280	+3.3	+4.9	+3.5	+5.1	Mediates the uptake of a variety of divalent cations including Fe^{2+}
DEGs in 3 out of 4 mutants							
HIPP39	Heavy metal-associated isoprenylated plant protein 39	Pop_G17G072830	ns	+11.0	+11.0	+11.5	Metallochaperones are key proteins for the transport of metallic ions inside the cell
SGT1	Protein SGT1 homolog	Pop_A17G034396	ns	+5.7	+5.3	+5.3	SGT1 specifically binds to the HSP90 chaperone and this core complex positively regulates plant developmental responses to Auxin and disease resistance
FRL4a	FRIGIDA-like protein 4a	Pop_A08G046246	ns	−10.0	−6.3	−4.7	The FRIGIDA (FRI) protein is associated to creating flowering time diversity in *Arabidopsis*
UGT88A1	UDP-glycosyltransferase 88A1	Pop_A17G034401	ns	+10.2	+11.1	+9.4	Involved in biosynthesis of quercetin, which is a powerful antioxidant that can mitigate biotic and abiotic stresses
F23H24	Trafficking protein particle complex subunit	Pop_A17G034397	ns	+9.0	+9.5	+9.0	SNARE-like protein involved in vesicle-mediated transport and vesicle fusion
VIT4	Vacuolar iron transporter homolog 4	Pop_G02G065539	+2.4	ns	−3.6	+2.6	Transports cytoplasmic Fe^{2+} (and putatively also other transition metal ions) into vacuoles
F6H1	Feruloyl CoA ortho-hydroxylase 1	Pop_A01G005912	+9.2	+10.4	ns	+12.5	Involved in biosynthesis of coumarins (e.g. scopoletin), which mobilize Fe previously bound to negatively charged cell wall
FRO2	Ferric reduction oxidase 2	Pop_G14G023596	+5.4	+5.1	ns	+5.7	Reduction of Fe^{3+} to Fe^{2+}, to facilitate the uptake from root medium into plant tissue

The false discovery rate (FDR) for significant differences was set to < 0.05, and no log_2FC filter was applied. The Venn diagram shows the uniquely expressed and shared genes of the different mutants after comparison to the wild-type and then to each other. The table focuses on the differentially expressed genes which were shared between all four or three out of four suberin mutants. Some outstanding genes were additionally and independently confirmed by an RT-qPCR analysis (Supporting Information Fig. S5). $n = 3$. log_2FC, log_2 fold change; red/+, significant up-regulation; blue/−, significant down-regulation; ns, not significant.

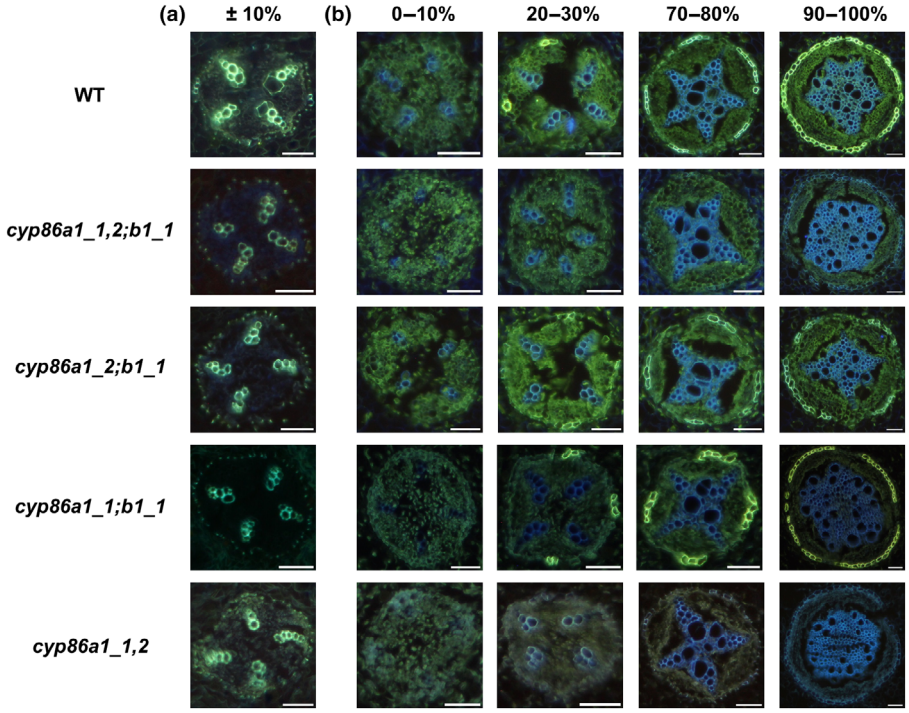

Fig. 2 Histochemical root analysis of the *Populus* × *canescens* wild-type (WT) and four suberin mutants after 5 wk of cultivation in hydroponics. Endodermal Casparian band development (a) was investigated with berberine-aniline blue at *c.* 10% relative distance behind the root tip. Endodermal suberin lamellae deposition (b) was investigated with fluorol yellow 088 at four different relative increments (0–10%, 20–30%, 70–80%, and 90–100%) divided throughout the whole root (the steadily increasing SL deposition between 20–30% and 70–80% was sporadically confirmed at 50% root length in some roots). A relative distance of 0% represents the root tip and 100% the root base. Based on observations of the WT, a functional zone of no suberization (Zone A, 0–21.5%) and patchy suberization (Zone B, 21.5–100%) was defined for analytical investigations. No exodermis formation or periderm formation has been observed in any line, and thus only the central cylinder is shown. Since the endodermis of *cyp86a1_1,2;b1_1* and *cyp86a1_1,2* could not be stained with fluorol yellow 088, a blue auto-fluorescence (see especially 90–100% in (b)) of the endodermis, indicating the deposition of aromatic constituents, is visible. $n \geq 6$. Bars, 100 μm.

Also, the chlorophyll content and stomatal conductance of leaves (Fig. 1c), the relative water content of roots and shoots (Fig. 1d), and the macronutrient concentration of leaves (Fig. 1e) were not considerably altered in most instances. The only striking differences in some of the mutants, when compared to the WT, appeared in the micronutrients iron (Fe), and potentially manganese (Mn) and zinc (Zn) (Fig. 1f).

Casparian band and suberin lamellae development

Irrespective of the putative suberin impairment suggested after the first analytical screening (Fig. S2), the CBs of all mutants developed like the WT. Already very close behind the root tip at *c.* 10% distance, the central cylinder with the first developing xylem elements was surrounded by an endodermis exhibiting CBs (Fig. 2a). In strong contrast to the CBs, the SL development of the roots was remarkably altered. In the WT, the onset of endodermal suberization localized at *c.* 21.5% relative distance, resulting in the definition of a non-suberized Zone A (0–21.5%). This endodermal suberization continued in a non-continuous but steadily increasing manner to the base (Zone B, patchy suberization, 21.5–100%) of the root (Fig. 2b). The mutants *cyp86a1_2;b1_1* and *cyp86a1_1;b1_1* exhibited a comparable onset of endodermal suberization, but the subsequent patchy suberized zone appeared to have slightly lower or delayed SL formation. The strongest contrast to the WT was observed in both mutants *cyp86a1_1,2;b1_1* and *cyp86a1_1,2*. Here, no suberin could be histochemically detected in any of the investigated increments using fluorol yellow 088, but a blue auto-fluorescence of the endodermis was visible where normally suberized cells would have been expected (see especially 90–100% in Fig. 2b). This blue auto-fluorescence is also visible in non-stained WT roots (no figure shown). No CBs or SL have been observed in the hypodermis of any roots, and thus, no exodermis was formed at any point during these experiments. In addition, a transition of adventitious roots in their primary developmental stage into the secondary formation of periderm tissue has never been observed within 5 wk of hydroponic cultivation.

Root suberin composition and amount

When the screening (Fig. S2) was repeated with a larger sample size and the subdivision of roots into functional Zones A and B, the histochemically observed phenotypes could be further confirmed by analytical data (Fig. 3). The suberin diagnostic functional groups of ω-OH acids and α,ω-diacids (those synthesized by the targeted enzymes CYP86A1 and CYP86B1) were reduced especially strong in the patchy suberized Zone B and by as much as 80–90% in the two phenotypically most striking mutants *cyp86a1_1,2;b1_1* and *cyp86a1_1,2* (Fig. 3a). The remaining functional groups of acids, alcohols, and 2-OH acids were not consistently altered (Fig. 3b). Considering the effects on absolute and relative amounts of all functional groups and chain-lengths observed in both root zones (Fig. S3), the chemical analysis revealed a suberin phenotype gradient of all mutants (WT>*cyp86a1_1;b1_1*>*cyp86a1_2;b1_1*>*cyp86a1_1,2*>*cyp86a1_1,2;b1_1*), with mutant *cyp86a1_1,2;b1_1* and *cyp86a1_1,2* being affected by far the most. In contrast to the aliphatic suberin fraction, the aromatic suberin fraction (Fig. S4a) and also co-released aromatic benzoic acid derivatives (Fig. S4b) did not allow drawing clear correlations.

Transport of water and solutes

To evaluate the effects of the observed suberin impairments on plant water and solute transport physiology, different

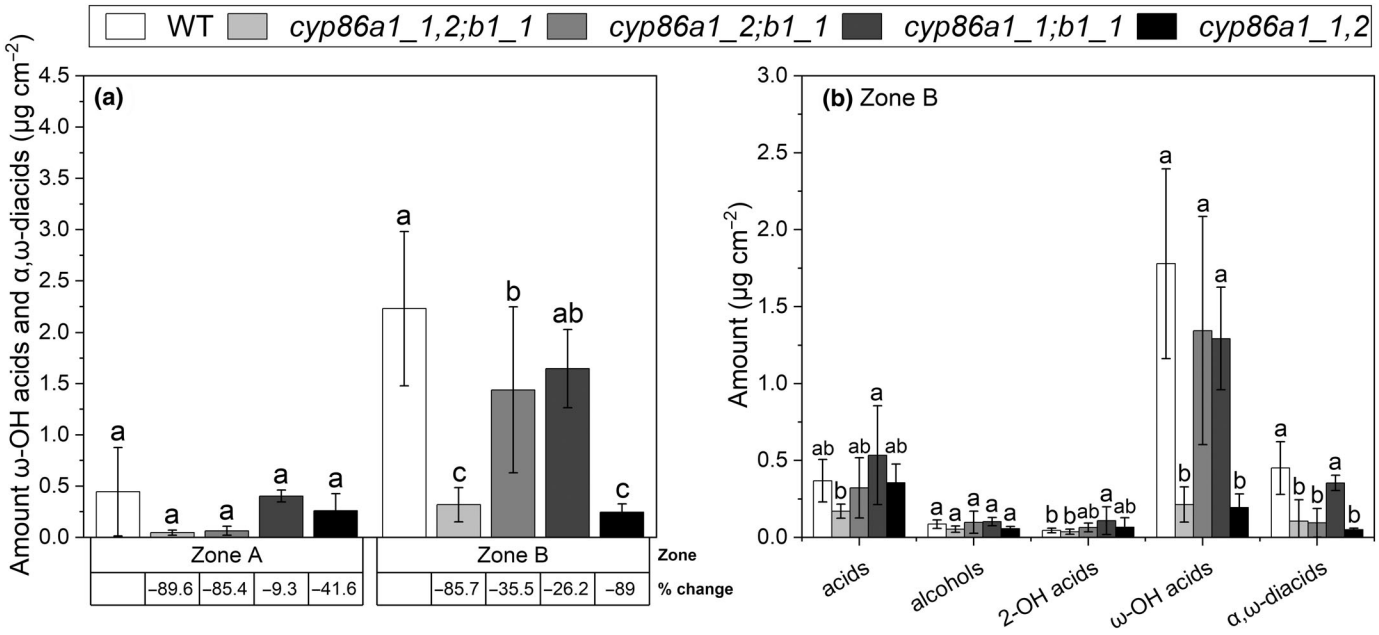

Fig. 3 Chemical root analysis of the *Populus* × *canescens* wild-type (WT) and four suberin mutants after 5 wk of cultivation in hydroponics. The amount of the suberin diagnostic functional groups ω-OH acids and α,ω-diacids divided into Zone A and Zone B (a) and all aliphatic functional groups of suberin in Zone B (b) are compared. Suberin amounts were related to the endodermal surface area. Means with SD ($n = 3$–8) are shown, and differential letters indicate significant (one-way ANOVA with Fisher's LSD *post hoc* test) differences at $P < 0.05$. acids, primary acids; alcohols, primary alcohols; 2-OH acids, 2-hydroxy acids; ω-OH acids, ω-hydroxy acids; α,ω-diacids, α,ω-dicarboxylic acids.

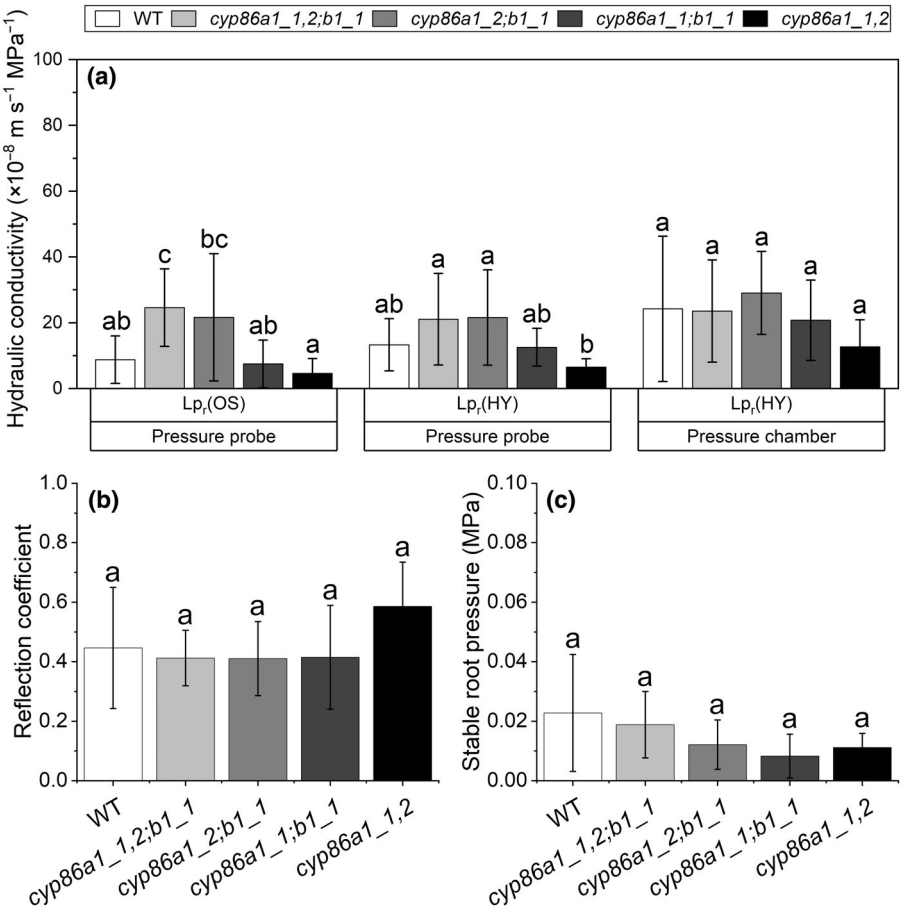

Fig. 4 Root water and nutrient ion transport properties of the *Populus* × *canescens* wild-type (WT) and four suberin mutants after 5 wk of cultivation in hydroponics. The osmotic hydraulic conductivity $Lp_r(OS)$ and the hydrostatic hydraulic conductivity $Lp_r(HY)$ were evaluated with two independent methods, the pressure probe and the pressure chamber (a). The pressure probe also allowed the investigation of the reflection coefficient of nutrient ions using a 5× concentrated ½ Hoagland solution (b) and the stable root pressure (c). Due to very low volumes of xylem sap exuding without applied pneumatic pressure, the $Lp_r(OS)$ could not be investigated with the pressure chamber. Means with standard deviations ($n = 6$–15) are shown, and differential letters indicate significant (one-way ANOVA with Fisher's LSD *post hoc* test) differences at $P < 0.01$. $Lp_r(OS)$, osmotic hydraulic conductivity; $Lp_r(HY)$, hydrostatic hydraulic conductivity.

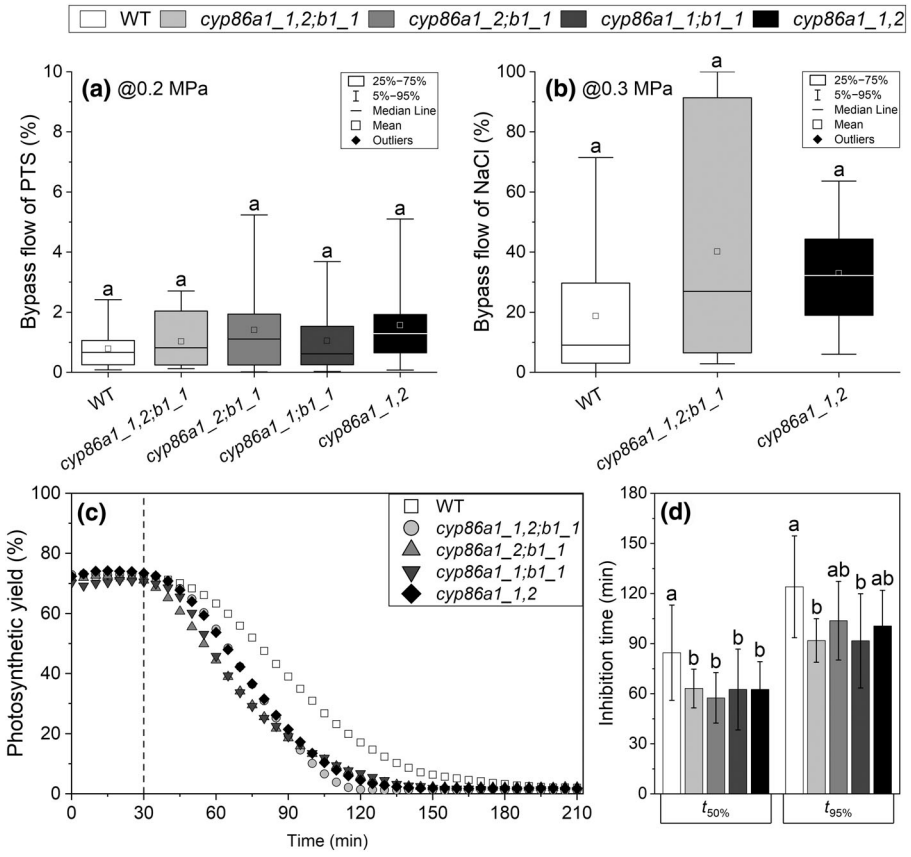

Fig. 5 Root and shoot solute transport properties of the *Populus* × *canescens* wild-type (WT) and four suberin mutants after 5 wk of cultivation in hydroponics. The bypass flow of PTS (a) and NaCl (b) at applied pneumatic pressures (0.01% (w/v) PTS at 0.2 MPa in (a), 50 mM NaCl at 0.3 MPa in (b), using the pressure chamber) as well as the decline of photosynthetic yield after photosynthesis inhibitor application to the roots (c) and the resulting yield inhibition times (d) are compared. In (a, b), different external pressures had to be used, because with the 0.2 MPa used for PTS, no measurements could be obtained for NaCl and only a higher pressure of 0.3 MPa was effective. In (b), only the WT and the two phenotypically most affected mutants (*cyp86a1_1,2;b1_1* and *cyp86a1_1,2*) were analyzed. Boxplots or means with or without (in c, SD were not shown to increase visibility) SD ($n = 7$–15 (a, b), 6–10 (c, d)) are shown, and differential letters indicate significant (Kruskal–Wallis ANOVA (a, b) and one-way ANOVA with Fisher's LSD *post hoc* test (d)) differences at $P < 0.01$ (a, b) or $P < 0.05$ (c, d). Dashed line in (c), application of photosynthesis inhibitor; $t_{50\%}$, 50% yield inhibition time; $t_{95\%}$, 95% yield inhibition time. The boxplots designate: box = 25–75%, whisker = 5–95%, horizontal line = median, empty square = mean, filled diamond = outlier.

experiments were performed with all mutants (Figs 4, 5). When measuring individual roots (pressure probe) as well as whole root systems (pressure chamber), it was found that neither the osmotic (Lp_r(OS)) nor the hydrostatic (Lp_r(HY)) conductivity of roots for water was altered consistently with the observed suberin phenotype (Fig. 4a). The Lp_r(OS) of the whole root system could not be measured with the pressure chamber because exuding xylem sap volumes were too close to the detection limit of the method. Also, using the pressure probe, the combined reflection coefficient of all nutrient ions (Fig. 4b) and the stable root pressure (Fig. 4c) were found not to be affected.

Both bypass flow experiments using the pressure chamber had to be performed at different external pressures because with the 0.2 MPa used for PTS, no measurements could be obtained for NaCl and only a higher pressure of 0.3 MPa was effective. The bypass flow of the large fluorescent tracer PTS was not statistically different for all investigated mutants (Fig. 5a), but the bypass flow of the smaller NaCl indicated a clear but not significant trend of being about twofold higher in *cyp86a1_1,2;b1_1* and *cyp86a1_1,2* than in the WT (Fig. 5b).

After application of Metribuzin to the roots, the decline of photosynthetic yield in the leaves was faster in all mutants when compared to the WT (Fig. 5c). And thus, the resulting $t_{50\%}$ and $t_{95\%}$ photosynthesis inhibition times were significantly lower in almost all cases (Fig. 5d).

Transcriptomic changes

To investigate the potential influence of the mutation-induced suberin deficiency on the overall gene expression already during non-stress conditions, root samples comprising the onset of SL development in the WT (20–50% relative root length) were harvested and analyzed using an RNA-sequencing approach. When the transcriptomes of all mutants were compared to that of the WT and subsequently to each other (Notes S3), a consistent set of only four genes (*S8H*, *FRO2*, 2× *IRT1*) was differentially expressed in all four mutants. These four DEGs and some additional genes only differentially expressed in three out of the four mutants could clearly be attributed to an iron (or divalent cation or metallic ion) metabolism pathway (Table 2). The observed expression changes in seven selected genes were independently confirmed by an reverse transcription quantitative polymerase chain reaction (Fig. S5). Interestingly, out of the eight *CYP86A1* and *CYP86B1* target gene orthologs and alleles (Fig. S1), one *CYP86B1_1* allele was found to be strongly down-regulated in mutant *cyp86a1_1,2;b1_1*, and one *CYP86B1_2* allele was strongly up-regulated in mutant *cyp86a1_1;b1_1* (Table S1).

Prolonged period of cultivation

A prolonged 7-wk-long hydroponic cultivation was carried out to obtain more mature (including full endodermal suberization and

periderm formation) roots exhibiting less non-suberized passage cells, because this should emphasize the effects of the mutation-induced suberin deficiency, especially in a transport physiological context. After 7 wk, the root lengths of the *cyp86a1_1,2;b1_1* mutant were significantly shorter (Fig. 6a) compared with the WT, but the shoot lengths (Fig. 6a), osmotic potentials of roots or leaves (Fig. 6b), and the chlorophyll content of leaves (Fig. 6c) were still very similar to that of the WT. Comparably to 5 wk of cultivation in hydroponics (Fig. 2b), even in 7-wk-old roots of the mutant *cyp86a1_1,2;b1_1*, no suberin could be histochemically detected in any of the investigated increments (Fig. 6d). But by strong contrast, in addition to the previously identified (Fig. 2b) functional zone of no suberization (here: Zone A, 0–20%) and patchy suberization (here: Zone B, 20–50%), roots of the WT now also exhibited a pronounced zone of full suberization (Zone C, 50–70%) and even showed a clear periderm development (Zone D, 70–100%) in the basal half of the root (Fig. 6e). The same four functional zones, even though the roots were shorter and not visibly suberized, could be identified in the mutant *cyp86a1_1,2;b1_1* (Fig. 6e). Again, analytical data confirmed these histochemically observed phenotypes and revealed reductions in the suberin diagnostic functional groups of ω-OH acids and α,ω-diacids in the mutant *cyp86a1_1,2;b1_*1 by as much as 80–95% on average (Fig. 6f), as well as pronounced compositional shifts when all functional groups or chain-lengths were compared (Fig. S6). In strong contrast to 5-wk-old whole root systems (Fig. 4a), the hydrostatic hydraulic conductivity of 7-wk-old root systems of the mutant *cyp86a1_1,2;b1_1* was significantly lower by > 50% on average (Fig. 6g).

Discussion

When root apoplastic barrier mutants of *Arabidopsis* became available (Beisson *et al.*, 2007; Höfer *et al.*, 2008; Baxter *et al.*, 2009; Compagnon *et al.*, 2009; Franke *et al.*, 2009; Lee *et al.*, 2009; Domergue *et al.*, 2010; Roppolo *et al.*, 2011), first analyses of root water and solute transport properties were carried out with *esb1* and *cyp86a1* in 2011 (Ranathunge & Schreiber, 2011). However, at that time, *esb1* was only known for its enhanced suberin deposition (Baxter *et al.*, 2009) and not yet for its defects in CB development (Hosmani *et al.*, 2013; Pfister *et al.*, 2014; Li *et al.*, 2017) and concomitant alterations in aquaporin activity (Wang *et al.*, 2019). Just recently, these early transport physiological investigations have been expanded with currently available and new *Arabidopsis* mutants being affected primarily in CB formation (Reyt *et al.*, 2021), SL deposition (Shukla *et al.*, 2021), or also combinations of both (Calvo-Polanco *et al.*, 2021). The conclusions drawn are partially conflicting, as some datasets seem to indicate a contribution of endodermal SL to water barrier properties, and others seem to reject this possibility. Also, in regard to the influence of SL on the ion fluxes, discrepancies prevail due to insignificant leaf ionome alterations in one study and remarkable changes in the other (see categories C=S- and C=S+ of Table 1). This might, in part, be due to significant differences in plant ages and cultivation conditions. While some studies focused on the primary roots of only few-day-old *Arabidopsis* seedlings, others investigated the well-developed whole root systems of mature plants of 3–5 wk of age, which certainly exhibited a secondarily developing periderm (Franke *et al.*, 2005; Höfer *et al.*, 2008).

In this study, we focused on adventitious roots in their primary developmental stage and specifically complemented this data with that of older roots exhibiting secondary periderm formation.

Plant development

Similar to earlier findings with *cyp86a1* and *cyp86b1* (Höfer *et al.*, 2008; Compagnon *et al.*, 2009) as well as with *quad-myb* (Shukla *et al.*, 2021) of *Arabidopsis*, our four mutants showed a development in the early stages of growth which was very comparable to that of the WT (Figs 1a–d, 6a–c). The CB formation has been observed in conjunction with the development of early xylem vessels (Fig. 2a), and the RNA-sequencing did not indicate any perturbations in genes related to CB biosynthesis. Furthermore, irrespective of the debate about suberin being a component of CBs, the CBs in the poplar mutants were proven functional by restricting the apoplastic bypass of PTS (Fig. 5a; Ranathunge & Schreiber, 2011). Unlike with *esb1* of *Arabidopsis* (Calvo-Polanco *et al.*, 2021), simultaneous functional alterations in both apoplastic barriers (CBs and suberin) can thus be ruled out.

These four poplar mutants appear to be affected exclusively in the suberin biosynthesis, which could already be deduced by histochemistry since suberin staining was not even possible in two of the four mutants (Figs 2b, 6d). Here, only the blue autofluorescence in endodermal cell walls was remaining (see especially 90–100% in Fig. 2b), indicating the deposition of aromatic constituents such as the negligibly small fraction of aromatic suberin or higher amounts of benzoic acid derivatives in poplar roots (Grünhofer *et al.*, 2021; Fig. S4). This auto-fluorescence is also visible in non-stained WT roots and, relying on the analysis of aromatic compounds (Fig. S4), does not seem to indicate a compensation mechanism of the two phenotypically most affected mutants (*cyp86a1_1,2;b1_1* and *cyp86a1_1,2*). It appears that the ontogenetic root developmental program (root cell elongation, differentiation, and maturation) is executed as usual, even in the strongest suberin phenotype mutants, but due to defects in the suberin biosynthesis pathway, only SL deposition is reduced.

Chemical analysis of suberin amounts confirmed the histochemical observations and showed that the mutants were gradually affected in endodermal or peridermal suberin content (WT>*cyp86a1_1;b1_1*>*cyp86a1_2;b1_1*>*cyp86a1_1,2*>*cyp86a1_1,2;b1_1*) with two mutants (*cyp86a1_1,2;b1_1* and *cyp86a1_1,2*) showing a decrease in zone-dependent suberization of up to 80–95% (Figs 3, S3, 6f, S6). Not all of the eight targeted orthologs and alleles were mapped in the RNA-sequencing analysis (Table S1), which might either result from the induced mutation or, more probably, from the chosen sequencing technology. The strong down-regulation of one *CYP86B1_1* allele in mutant *cyp86a1_1,2;b1_1* might indeed be a consequence of the gene editing. Instead, the observed strong up-regulation of one *CYP86B1_2* allele in mutant *cyp86a1_1;b1_1* could potentially explain why the root suberin of this mutant is most similar in

amount and composition to that of the WT (Figs 3, S3). This might thus indicate a genetic compensation that is not observed in any of the other mutants.

According to the latest version of the genome annotation of *P. trichocarpa* (https://phytozome-next.jgi.doe.gov/info/Ptrichocarpa_v4_1; Tuskan *et al.*, 2006), there are eight members in the *CYP86* gene family (Table S2) of which only *CYP86A1* and *CYP86B1* are known to participate in the suberin biosynthesis pathway (Ranathunge *et al.*, 2011b; Vishwanath *et al.*, 2015; Serra & Geldner, 2022). Some of the remaining genes were found to be significantly up-regulated in cork formation (Rains *et al.*, 2017), but could not be identified in our RNA-sequencing analysis.

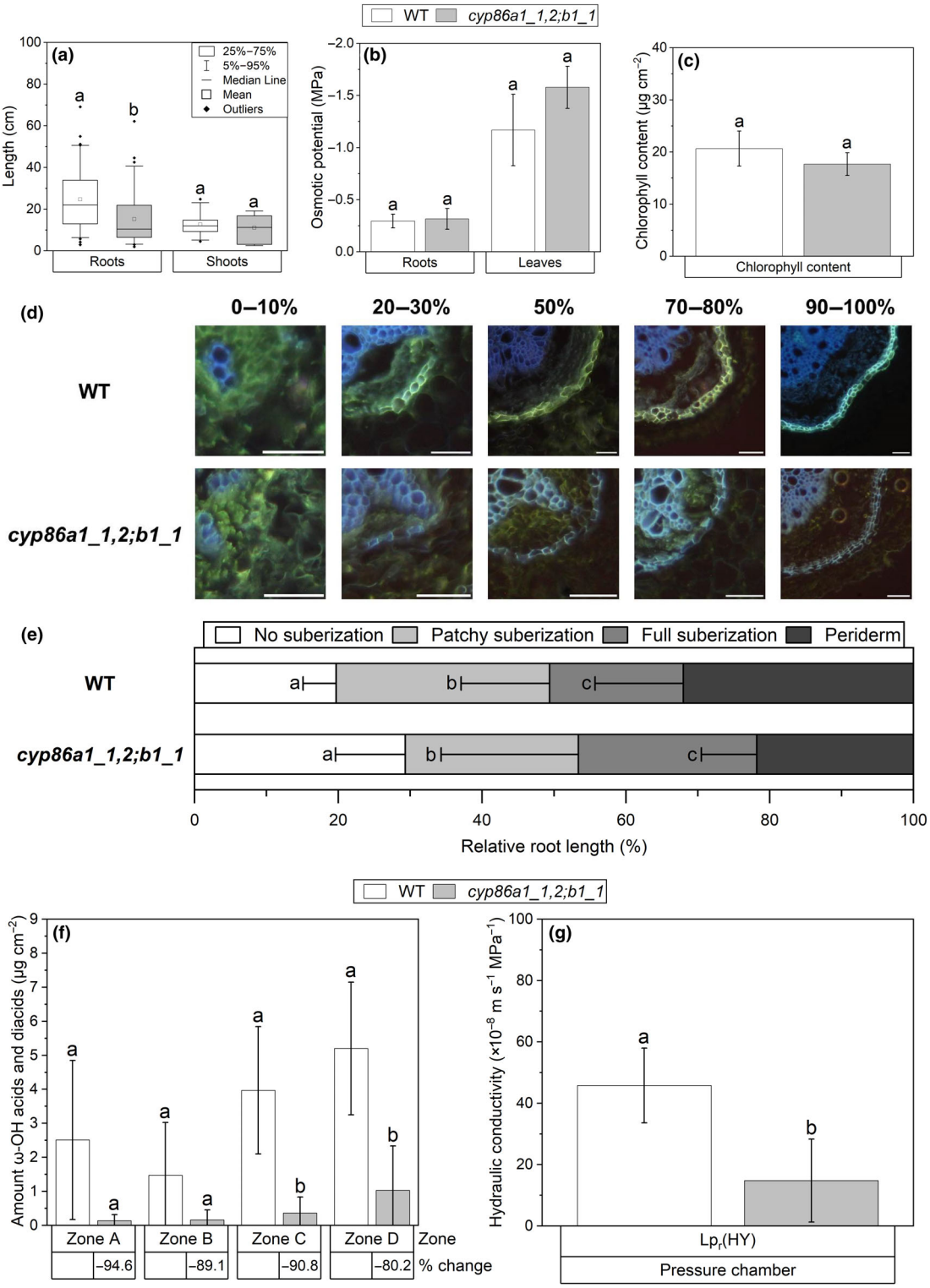

Fig. 6 Selected experiments additionally investigating the *Populus* × *canescens* wild-type (WT) and the most affected mutant (*cyp86a1_1,2;b1_1*) after a prolonged period of 7 wk of cultivation in hydroponics. Root and shoot length (a), osmotic potentials of roots and leaves (b), chlorophyll content of leaves (c), endodermal or peridermal suberin lamellae deposition (d, e), the amount of the suberin diagnostic functional groups ω-OH acids and α,ω-diacids (f), and the hydrostatic hydraulic conductivity Lp_r(HY) evaluated with the pressure chamber (g) are compared. In (d), suberin lamellae deposition was investigated with fluorol yellow 088 at five different relative increments (0–10%, 20–30%, 50%, 70–80%, and 90–100%) divided throughout the whole root. A relative distance of 0% represents the root tip and 100% the root base. Since no exodermis formation has been observed in any line and the periderm originates from the pericycle beneath the endodermis, the outer tissue layers have been cropped to increase visibility. Since the endodermis and periderm of *cyp86a1_1,2;b1_1* could not be stained with fluorol yellow 088, a blue auto-fluorescence of the endodermis and periderm, indicating the deposition of aromatic constituents, is visible. Bars, 100 μm. In (e), observations of the root development of the WT were used to define functional zones of no suberization (Zone A, 0–20%), patchy suberization (Zone B, 20–50%), full suberization (Zone C, 50–70%), and suberized periderm (Zone D, 70–100%) for analytical investigations. In (f), roots were divided into the functional zones A, B, C, and D, and suberin amounts were related to the endodermal or peridermal surface area. In (g), the Lp_r(OS) could not be investigated with the pressure chamber due to very low volumes of xylem sap exuding without applied pneumatic pressure. Boxplots or means with standard deviations ($n = 62$–98 roots and 10–20 shoots (a), 4 (b, c), ≥ 6 (d, e), 3–4 (f), 6–7 (g)) are shown, and differential letters indicate significant (Kruskal–Wallis ANOVA (a) and one-way ANOVA with Fisher's LSD *post hoc* test (b, c, e–g)) differences at $P < 0.05$ (a–c, e, f) or $P < 0.01$ (g). ω-OH acids, ω-hydroxy acids; α,ω-diacids, α,ω-dicarboxylic acids; Lp_r(OS), osmotic hydraulic conductivity; Lp_r(HY), hydrostatic hydraulic conductivity. The boxplots designate: box = 25–75%, whisker = 5–95%, horizontal line = median, empty square = mean, filled diamond = outlier.

Conversely, aside from *CYP86A1* and *CYP86B1*, only two more CYPs are currently described to participate in the suberin biosynthesis pathway in *Arabidopsis* (Table S2). The *P. trichocarpa* ortholog of both genes could be identified in our RNA-sequencing analysis, but was not significantly differentially regulated.

Taken together, these poplar mutants fall into the category C=S- (functional CBs and reduced SL deposition) suggested by Calvo-Polanco *et al.* (2021), which means that the transport physiological findings should exclusively be attributable to functional defects of the SL or secondarily induced compensation mechanisms. While the radial flow of water from the root medium to the xylem vessels is driven by both osmotic (Lp_r(OS)) and hydrostatic (Lp_r(HY)) pressure gradients, the longitudinal transport in xylem vessels is primarily affected by hydrostatic driving forces. On the other hand, both radial and longitudinal transport of solutes depends on concentration gradients, contributions of transporters, electric fields, and convection. Thus, water and solute transport are to some degree interdependent because water flux affects the convection of solutes, and solutes, in turn, modulate the osmotic forces driving water transport (Foster & Miklavcic, 2016).

Water transport physiology

While Ranathunge & Schreiber (2011) and Calvo-Polanco *et al.* (2021) found no differences in the water transport of *Arabidopsis* mutants with increased suberin amounts irrespective of the status of CB (C-S+ and C=S+), Reyt *et al.* (2021) identified the observed lower water transport to mainly originate from the reduction in aquaporin-mediated water transport as a consequence of defects in CB development (C-S+). Thus, based on the available data, higher amounts of suberin do not seem to directly decrease water transport. This is supported by modeling approaches concluding that a reduction of root water flow does not necessarily require additional apoplastic hydraulic resistances, including SL, but that this can be sufficiently fulfilled by the activity and gene expression level of aquaporins (Knipfer *et al.*, 2021). The situation appears more complex in mutants with intact CBs but reduced amounts or shifted composition of root suberin (C=S- and C=Sx). Here, osmotically as well as hydrostatically driven water flow was higher in *Arabidopsis* mutants with lower suberin amounts (Ranathunge & Schreiber, 2011; Calvo-Polanco *et al.*, 2021), but paradoxically highest in the mutant exhibiting WT levels of root suberin but only a shifted composition (C=Sx), even after considering the contribution of aquaporins (Calvo-Polanco *et al.*, 2021).

By contrast, our study did not detect a clear correlation between the decreased SL deposition and both osmotic and hydrostatic water flow (Fig. S7) even though the amount of non-suberized endodermal passage cells (Andersen *et al.*, 2018) was considerably higher after 5 wk of cultivation, at least in the mutants *cyp86a1_1,2;b1_1* and *cyp86a1_1,2*. It was verified with two independent methods examining both individual roots and whole root systems (Fig. 4a). The only significantly increased Lp_r of any mutant line in comparison with the WT (Lp_r(OS) of *cyp86a1_1,2;b1_1*) could not be confirmed by a concurrent significant increase in the Lp_r(OS) of the other most suberin-impaired mutant *cyp86a1_1,2*. In parallel, the less-affected mutant *cyp86a1_2;b1_1* also had a fairly high Lp_r(OS). We primarily interpret this as a consequence of the highly delicate root pressure probe method used, which can lead to large variability. But while previously having created an experimental pipeline ensuring a high degree of reliability and reproducibility (Grünhofer *et al.*, 2021), the observed variability might as well originate from the potentially unequal development of adventitious roots caused by the known relative independence of individual root primordia in poplar stems (Luxová & Lux, 1981). To even investigate a potential override of effects by the anyway pronounced prevalence of non-suberized passage cells even in the WT, significantly more matured 7-wk-old root systems of the WT and *cyp86a1_1,2;b1_1* were also measured with the pressure chamber. Although these roots of the WT now exhibited a functional zone of full suberization and even periderm formation in the basal half (Fig. 6e), the Lp_r(HY) was still not higher in the suberin-deficient mutant, but even significantly lower by about threefold (Fig. 6g). While being limited to speculations at this point, a theoretical indirect effect of the mutation on aquaporin expression (which was, however, not indicated by the RNA-sequencing data of 5-wk-old roots), or a potentially compensatory higher number of peridermal cell layers (Fig. 6d) might increase the radial resistance for water flow.

Taken together, three independent experimental approaches (pressure probe and pressure chamber after 5 wk, and pressure chamber after 7 wk; Figs 4a, 6g) support the hypothesis of less root suberin not increasing hydrostatic water transport. While minor increases in the osmotic water transport cannot unequivocally be ruled out for all mutants (Fig. 4a), it must be noted that especially in woody plants, the Lp_r(HY) can exert an up to three orders of magnitude higher contribution to the overall water transport (Steudle & Peterson, 1998). If root suberin is indeed not viewed as being the rate-limiting factor of hydrostatic water transport, the observed lower Lp_r(HY) of *cyp86a1_1,2;b1_1* after 7 wk (Fig. 6g) might also be caused by a smaller diameter of xylem vessels in the shorter (Fig. 6a) and slightly less developed (Fig. 6d,e) roots. Although xylem volume was not explicitly investigated, it is apparent that the Lp_r(HY) of 7-wk-old *cyp86a1_1,2;b1_1* roots is almost identical to that of 5-wk-old roots of any line, while the Lp_r(HY) of more matured 7-wk-old WT roots, potentially exhibiting larger xylem vessels, advanced to be about threefold higher (Figs 4a, 6g).

Since the abovementioned studies, including our own, were focused on plants in non-stress conditions, the situation can still be different during abiotic stress exposure. In a situation where stomatal transpiration is largely absent and bulk flow of water is minimized (no Lp_r(HY)), the water potential gradient directed outward during osmotic or salt stress could still be leading to a higher uncontrolled diffusional (Lp_r(OS)) loss of water in roots with less suberin (Su *et al.*, 2023).

Solute transport physiology

Although significantly decreased iron contents in leaves (Fig. 1f) were identified together with a significantly up-regulated iron deficiency response in roots (Table 2), a frequently coinciding (Marschner, 2012) decrease in chlorophyll content (Fig. 1c) or lower baseline photosynthetic yield (before the application of the herbicide; Fig. 5c) was not observed. Chlorosis was also never observed with the older plants (14–18 wk-old) growing on soil to initiate hydroponics. Thus, the up-regulation of *S8H*, *FRO2*, *IRT1*, etc. (Table 2), which is a common phenomenon observed in plants grown under iron deficiency, is obviously sufficient to compensate for the iron imbalances caused by the defective SL deposition. Dicotyledonous plants generally employ the iron strategy I to acquire iron from the root medium (Marschner & Römheld, 1994). This includes the excretion of protons and coumarins (involvement of *S8H*) to solubilize and chelate Fe^{3+}, the reduction in Fe^{3+} to Fe^{2+} by the ferric reduction oxidase *FRO2*, and ultimately the uptake of Fe^{2+} by the iron-regulated transporter *IRT1* (Curie & Mari, 2017; Jeong *et al.*, 2017). In both dicotyledonous plants, *Phaseolus vulgaris* (Sijmons *et al.*, 1985) and *Arabidopsis* (Barberon *et al.*, 2016), iron deficiency led to a decreased suberization of the roots, which was not the case for the monocot *Zea mays*, employing another iron uptake strategy (Sijmons *et al.*, 1985). It was argued that the unsuberized root zones where Fe^{3+} reduction can occur are elongated in iron deficiency conditions by exposing increased amounts of plasma membrane surface area for nutrient mobilization and uptake (Sijmons *et al.*, 1985). Thus, contrary to *Phaseolus*, the iron deficiency phenotype observed in this study (Fig. 1f; Table 2) might be a consequence of the reduced endodermal SL deposition. The lack of a suberized barrier leading to reduced masking of plasma membrane surface area (Ranathunge & Schreiber, 2011; Redjala *et al.*, 2011) could result in enhanced or reduced uptake but also leakage (Enstone *et al.*, 2003; Chen *et al.*, 2019) of beneficial and also harmful solutes. The increased uptake and translocation of the photosynthesis inhibitor Metribuzin from the roots to the shoots (Fig. 5c,d) ties in very well with this idea. The endodermis, even without developed SL, has previously been shown to be the rate-limiting barrier for solutes but not water (Peterson *et al.*, 1993; Steudle *et al.*, 1993), and thus, a reduced masking of the plasma membrane as a consequence of the decreased SL deposition might indeed affect the solute transport dynamics.

However, the reflection coefficients for nutrient ions of the whole root were unaffected (Fig. 4b). This is attributed to the fact that all nutrient ions were investigated simultaneously, the endodermis and the remaining cortex were fully intact even in the mutants, the nutrient-specific transporters remained functional, and overall plant development was barely altered. But when exposing roots to PTS and NaCl, a trend of increased bypass (inwards leakage) of NaCl ions could be observed (Fig. 5a,b). Due to its size and charge PTS bypass does not reflect water flow, but it was suggested that it represents a good tracer for the transport of ions and organic solutes (Ranathunge & Schreiber, 2011). In this study using the roots of poplar, NaCl bypass was > 10-fold higher than PTS. This might partly be due to the higher pressure applied in the experiments. But in addition, the larger apoplastic tracer molecule PTS is described as not passing plasma membranes within adequate exposure times, which cannot be excluded for the significantly smaller NaCl ions potentially also traveling along the transmembrane pathway. These observations of higher NaCl bypass in suberin-deficient mutants (Fig. 5b) indeed fit well with previous reports of higher NaCl permeability in *cyp86a1* (Ranathunge & Schreiber, 2011), salt hypersensitivity of further decreased suberin mutants (Barberon *et al.*, 2016; Shukla *et al.*, 2021; Ursache *et al.*, 2021), and higher salt tolerance of increased suberin mutants (Krishnamurthy *et al.*, 2021) of *Arabidopsis*.

Taken together, these data again indicate the importance of SL in modulating especially the transcellular rather than the apoplastic transport pathway (Shukla *et al.*, 2021).

Acknowledgements

We thank Katrin Groppe (Thuenen Institute of Forest Genetics, Grosshansdorf) for performing the transformations, subsequent *in vitro* cultivations of putatively edited poplar lines, and PCR analyses. Thanks to Lena Herzig, Jorge Carvajal Vásquez, and Kiran Suresh for assisting in microscopy and plant harvests, and Kosala Ranathunge for discussing the data with us. The authors thank the NGS Core Facility of the Bonn University Hospital for performing the transcriptomic sequencing. Financial support by the Deutsche Forschungsgemeinschaft (DFG, German Research

Foundation; SCHR17/1; Project Number 391657309), the National Natural Science Foundation of China (31761133009), and the Programme of Introducing Talents of Discipline to Universities (111 project, B13007) is highly appreciated. Open Access funding enabled and organized by Projekt DEAL.

Competing interests

None declared.

Author contributions

LS and PG designed the experiments. IH, SP, MO, LZ, KL and PG performed the physiological experiments. PG and TS evaluated the transcriptomics data. HM and MF performed the molecular experiments. TK identified the genes of interest in poplar and assisted in ICP-OES analyses. PG and LS evaluated the data. PG wrote the manuscript. TS, HM, YG, RL, JL, MF, TK, SNHB, LZ, HS and LS revised the manuscript. All authors read and approved the final manuscript.

ORCID

Syed Nadeem Hussain Bokhari https://orcid.org/0000-0002-7446-8867
Matthias Fladung https://orcid.org/0000-0001-9301-8581
Paul Grünhofer https://orcid.org/0000-0002-6298-5656
Yayu Guo https://orcid.org/0000-0003-3196-2109
Tino Kreszies https://orcid.org/0000-0003-0236-9736
Ruili Li https://orcid.org/0000-0001-5112-3201
Jinxing Lin https://orcid.org/0000-0001-9338-1356
Hongjun Meng https://orcid.org/0009-0000-2524-101X
Heiko Schoof https://orcid.org/0000-0002-1527-3752
Lukas Schreiber https://orcid.org/0000-0001-7003-9929
Tyll Stöcker https://orcid.org/0000-0001-7184-9472
Lin Zi https://orcid.org/0000-0002-3300-4695

Data availability

The raw sequencing data have been deposited at the National Center for Biotechnology Information (NCBI) sequence read archive (SRA study: PRJNA940679).

References

Andersen TG, Naseer S, Ursache R, Wybouw B, Smet W, De Rybel B, Vermeer JEM, Geldner N. 2018. Diffusible repression of cytokinin signalling produces endodermal symmetry and passage cells. *Nature* **555**: 529–533.

Baales J, Zeisler-Diehl VV, Schreiber L. 2021. Analysis of extracellular cell wall lipids: wax, cutin, and suberin in leaves, roots, fruits, and seeds. In: Bartels D, Dörmann P, eds. *Plant lipids. Methods and protocols*. New York, NY, USA: Springer US; Humana, 275–293.

Bagniewska-Zadworna A, Stelmasik A, Minicka J. 2014. From birth to death – *Populus trichocarpa* fibrous roots functional anatomy. *Biologia Plantarum* **58**: 551–560.

Barberon M, Vermeer JEM, de Bellis D, Wang P, Naseer S, Andersen TG, Humbel BM, Nawrath C, Takano J, Salt DE. 2016. Adaptation of root function by nutrient-induced plasticity of endodermal differentiation. *Cell* **164**: 447–459.

Baxter I, Hosmani PS, Rus A, Lahner B, Borevitz JO, Muthukumar B, Mickelbart MV, Schreiber L, Franke RB, Salt DE. 2009. Root suberin forms an extracellular barrier that affects water relations and mineral nutrition in Arabidopsis. *PLoS Genetics* **5**: e1000492.

Beisson F, Li Y, Bonaventure G, Pollard M, Ohlrogge JB. 2007. The acyltransferase GPAT5 is required for the synthesis of suberin in seed coat and root of *Arabidopsis*. *Plant Cell* **19**: 351–368.

Brundrett MC, Enstone DE, Peterson CA. 1988. A berberine-aniline blue fluorescent staining procedure for suberin, lignin, and callose in plant tissue. *Protoplasma* **146**: 133–142.

Brundrett MC, Kendrick B, Peterson CA. 1991. Efficient lipid staining in plant material with sudan red 7B or fluoral yellow 088 in polyethylene glycol-glycerol. *Biotechnic & Histochemistry* **66**: 111–116.

Brunner I, Herzog C, Dawes MA, Arend M, Sperisen C. 2015. How tree roots respond to drought. *Frontiers in Plant Science* **6**: 547.

Calvo-Polanco M, Ribeyre Z, Dauzat M, Reyt G, Hidalgo-Shrestha C, Diehl P, Frenger M, Simonneau T, Muller B, Salt DE *et al.* 2021. Physiological roles of Casparian strips and suberin in the transport of water and solutes. *New Phytologist* **232**: 2295–2307.

Chen A, Husted S, Salt DE, Schjoerring JK, Persson DP. 2019. The intensity of manganese deficiency strongly affects root endodermal suberization and ion homeostasis. *Plant Physiology* **181**: 729–742.

Compagnon V, Diehl P, Benveniste I, Meyer D, Schaller H, Schreiber L, Franke R, Pinot F. 2009. CYP86B1 is required for very long chain omega-hydroxyacid and alpha, omega-dicarboxylic acid synthesis in root and seed suberin polyester. *Plant Physiology* **150**: 1831–1843.

Crang R, Lyons-Sobaski S, Wise R. 2018. *Plant anatomy. a concept-based approach to the structure of seed plants*. Cham, Switzerland: Springer.

Curie C, Mari S. 2017. New routes for plant iron mining. *New Phytologist* **214**: 521–525.

Domergue F, Vishwanath SJ, Joubès J, Ono J, Lee JA, Bourdon M, Alhattab R, Lowe C, Pascal S, Lessire R *et al.* 2010. Three Arabidopsis fatty acyl-coenzyme a reductases, FAR1, FAR4, and FAR5, generate primary fatty alcohols associated with suberin deposition. *Plant Physiology* **153**: 1539–1554.

Enstone DE, Peterson CA, Ma F. 2003. Root endodermis and exodermis: structure, function, and responses to the environment. *Journal of Plant Growth Regulation* **21**: 335–351.

Fladung M, Kumar S, Ahuja MR. 1997. Genetic transformation of *Populus* genotypes with different chimaeric gene constructs: transformation efficiency and molecular analysis. *Transgenic Research* **6**: 111–121.

Foster KJ, Miklavcic SJ. 2016. Modeling root zone effects on preferred pathways for the passive transport of ions and water in plant roots. *Frontiers in Plant Science* **7**: 914.

Franke R, Briesen I, Wojciechowski T, Faust A, Yephremov A, Nawrath C, Schreiber L. 2005. Apoplastic polyesters in *Arabidopsis* surface tissues – a typical suberin and a particular cutin. *Phytochemistry* **66**: 2643–2658.

Franke R, Höfer R, Briesen I, Emsermann M, Efremova N, Yephremov A, Schreiber L. 2009. The *DAISY* gene from Arabidopsis encodes a fatty acid elongase condensing enzyme involved in the biosynthesis of aliphatic suberin in roots and the chalaza-micropyle region of seeds. *The Plant Journal* **57**: 80–95.

Frensch J, Steudle E. 1989. Axial and radial hydraulic resistance to roots of maize (*Zea mays* L.). *Plant Physiology* **91**: 719–726.

Grünhofer P, Guo Y, Li R, Lin J, Schreiber L. 2021. Hydroponic cultivation conditions allowing the reproducible investigation of poplar root suberization and water transport. *Plant Methods* **17**: 129.

Grünhofer P, Heimerich I, Herzig L, Pohl S, Schreiber L. 2023. Apoplastic barriers of *Populus* × *canescens* roots in reaction to different cultivation conditions and abiotic stress treatments. *Stress Biology* **3**: 1–14.

Grünhofer P, Herzig L, Sent S, Zeisler-Diehl VV, Schreiber L. 2022a. Increased cuticular wax deposition does not change residual foliar transpiration. *Plant, Cell & Environment* **45**: 1157–1171.

Grünhofer P, Schreiber L. 2023. Cutinized and suberized barriers in leaves and roots: similarities and differences. *Journal of Plant Physiology* **282**: 153921.

Grünhofer P, Stöcker T, Guo Y, Li R, Lin J, Ranathunge K, Schoof H, Schreiber L. 2022b. *Populus* × *canescens* root suberization in reaction to osmotic and salt stress is limited to the developing younger root tip region. *Physiologia Plantarum* **174**: e13765.

Hanson PJ, Sucoff EI, Markhart AH. 1985. Quantifying apoplastic flux through red pine root systems using trisodium, 3-hydroxy-5,8,10-pyrenetrisulfonate. *Plant Physiology* **77**: 21–24.

Höfer R, Briesen I, Beck M, Pinot F, Schreiber L, Franke R. 2008. The *Arabidopsis* cytochrome P450 *CYP86A1* encodes a fatty acid omega-hydroxylase involved in suberin monomer biosynthesis. *Journal of Experimental Botany* **59**: 2347–2360.

Hosmani PS, Kamiya T, Danku J, Naseer S, Geldner N, Guerinot ML, Salt DE. 2013. Dirigent domain-containing protein is part of the machinery required for formation of the lignin-based Casparian strip in the root. *Proceedings of the National Academy of Sciences, USA* **110**: 14498–14503.

Jeong J, Merkovich A, Clyne M, Connolly EL. 2017. Directing iron transport in dicots: regulation of iron acquisition and translocation. *Current Opinion in Plant Biology* **39**: 106–113.

Kamiya T, Borghi M, Wang P, Danku JMC, Kalmbach L, Hosmani PS, Naseer S, Fujiwara T, Geldner N, Salt DE. 2015. The MYB36 transcription factor orchestrates Casparian strip formation. *Proceedings of the National Academy of Sciences, USA* **112**: 10533–10538.

Knipfer T, Danjou M, Vionne C, Fricke W. 2021. Salt stress reduces root water uptake in barley (*Hordeum vulgare* L.) through modification of the transcellular transport path. *Plant, Cell & Environment* **44**: 458–475.

Kreszies T, Schreiber L, Ranathunge K. 2018. Suberized transport barriers in *Arabidopsis*, barley and rice roots: from the model plant to crop species. *Journal of Plant Physiology* **227**: 75–83.

Kreszies T, Shellakkutti N, Osthoff A, Yu P, Baldauf JA, Zeisler-Diehl VV, Ranathunge K, Hochholdinger F, Schreiber L. 2019. Osmotic stress enhances suberization of apoplastic barriers in barley seminal roots: analysis of chemical, transcriptomic and physiological responses. *New Phytologist* **221**: 180–194.

Krishnamurthy P, Vishal B, Bhal A, Kumar PP. 2021. WRKY9 transcription factor regulates cytochrome P450 genes *CYP94B3* and *CYP86B1*, leading to increased root suberin and salt tolerance in Arabidopsis. *Physiologia Plantarum* **172**: 1673–1687.

Lee S-B, Jung S-J, Go Y-S, Kim H-U, Kim J-K, Cho H-J, Park OK, Suh M-C. 2009. Two Arabidopsis 3-ketoacyl CoA synthase genes, *KCS20* and *KCS2/DAISY*, are functionally redundant in cuticular wax and root suberin biosynthesis, but differentially controlled by osmotic stress. *The Plant Journal* **60**: 462–475.

Leplé J-C, Brasileiro ACM, Michel MF, Delmotte F, Jouanin L. 1992. Transgenic poplars: expression of chimeric genes using four different constructs. *Plant Cell Reports* **11**: 137–141.

Li B, Kamiya T, Kalmbach L, Yamagami M, Yamaguchi K, Shigenobu S, Sawa S, Danku JMC, Salt DE, Geldner N *et al.* 2017. Role of *LOTR1* in nutrient transport through organization of spatial distribution of root endodermal barriers. *Current Biology* **27**: 758–765.

Luxová M, Lux A. 1981. The course of root differentiation from root primordia in poplar stems. *Biologia Plantarum* **23**: 401–405.

Mader M, Le Paslier M-C, Bounon R, Bérard A, Rampant PF, Fladung M, Leplé J-C, Kersten B. 2016. Whole-genome draft assembly of *Populus tremula* × *P. alba* clone INRA 717-1B4. *Silvae Genetica* **65**: 74–79.

Marschner H. 2012. *Mineral nutrition of higher plants*. Amsterdam, the Netherlands: Academic Press.

Marschner H, Römheld V. 1994. Strategies of plants for acquisition of iron. *Plant and Soil* **165**: 261–274.

Miyamoto N, Steudle E, Hirasawa T, Lafitte R. 2001. Hydraulic conductivity of rice roots. *Journal of Experimental Botany* **52**: 1835–1846.

Nobel PS. 2020. *Physicochemical and environmental plant physiology*. London, UK: Academic Press.

Peterson C, Murrmann M, Steudle E. 1993. Location of the major barriers to water and ion movement in young roots of *Zea mays* L. *Planta* **190**: 127–136.

Pfister A, Barberon M, Alassimone J, Kalmbach L, Lee Y, Vermeer JEM, Yamazaki M, Li G, Maurel C, Takano J *et al.* 2014. A receptor-like kinase mutant with absent endodermal diffusion barrier displays selective nutrient homeostasis defects. *eLife* **3**: e03115.

Qiu D, Bai S, Ma J, Zhang L, Shao F, Zhang K, Yang Y, Sun T, Huang J, Zhou Y *et al.* 2019. The genome of *Populus alba* × *Populus tremula* var. *glandulosa* clone 84K. *DNA Research* **26**: 423–431.

R Core Team. 2023. *R: a language and environment for statistical computing*. Vienna, Austria: R Foundation for Statistical Computing. [WWW document] URL https://www.r-project.org/ [accessed 5 November 2023].

Rains MK, Gardiyehewa de Silva ND, Molina I. 2017. Reconstructing the suberin pathway in poplar by chemical and transcriptomic analysis of bark tissues. *Tree Physiology* **38**: 340–361.

Ranathunge K, Kim YX, Wassmann F, Kreszies T, Zeisler V, Schreiber L. 2017. The composite water and solute transport of barley (*Hordeum vulgare*) roots: effect of suberized barriers. *Annals of Botany* **119**: 629–643.

Ranathunge K, Lin J, Steudle E, Schreiber L. 2011a. Stagnant deoxygenated growth enhances root suberization and lignifications, but differentially affects water and NaCl permeabilities in rice (*Oryza sativa* L.) roots. *Plant, Cell & Environment* **34**: 1223–1240.

Ranathunge K, Schreiber L. 2011. Water and solute permeabilities of *Arabidopsis* roots in relation to the amount and composition of aliphatic suberin. *Journal of Experimental Botany* **62**: 1961–1974.

Ranathunge K, Schreiber L, Franke R. 2011b. Suberin research in the genomics era – new interest for an old polymer. *Plant Science* **180**: 399–413.

Redjala T, Zelko I, Sterckeman T, Legué V, Lux A. 2011. Relationship between root structure and root cadmium uptake in maize. *Environmental and Experimental Botany* **71**: 241–248.

Reyt G, Ramakrishna P, Salas-González I, Fujita S, Love A, Tiemessen D, Lapierre C, Morreel K, Calvo-Polanco M, Flis P *et al.* 2021. Two chemically distinct root lignin barriers control solute and water balance. *Nature Communications* **12**: 2320.

Robinson MD, McCarthy DJ, Smyth GK. 2010. edgeR: a Bioconductor package for differential expression analysis of digital gene expression data. *Bioinformatics* **26**: 139–140.

Roppolo D, De Rybel B, Dénervaud Tendon V, Pfister A, Alassimone J, Vermeer JEM, Yamazaki M, Stierhof Y-D, Beeckman T, Geldner N. 2011. A novel protein family mediates Casparian strip formation in the endodermis. *Nature* **473**: 380–383.

Schönherr J, Lendzian K. 1981. A simple and inexpensive method of measuring water permeability of isolated plant cuticular membranes. *Zeitschrift für Pflanzenphysiologie* **102**: 321–327.

Schreiber L, Franke R, Hartmann K. 2005a. Wax and suberin development of native and wound periderm of potato (*Solanum tuberosum* L.) and its relation to peridermal transpiration. *Planta* **220**: 520–530.

Schreiber L, Franke R, Hartmann K-D, Ranathunge K, Steudle E. 2005b. The chemical composition of suberin in apoplastic barriers affects radial hydraulic conductivity differently in the roots of rice (*Oryza sativa* L. cv. IR64) and corn (*Zea mays* L. cv. Helix). *Journal of Experimental Botany* **56**: 1427–1436.

Schreiber L, Hartmann K, Skrabs M, Zeier J. 1999. Apoplastic barriers in roots: chemical composition of endodermal and hypodermal cell walls. *Journal of Experimental Botany* **50**: 1267–1280.

Serra O, Geldner N. 2022. The making of suberin. *New Phytologist* **235**: 848–866.

Shukla V, Barberon M. 2021. Building and breaking of a barrier: suberin plasticity and function in the endodermis. *Current Opinion in Plant Biology* **64**: 102153.

Shukla V, Han J-P, Cléard F, Lefebvre-Legendre L, Gully K, Flis P, Berhin A, Andersen TG, Salt DE, Nawrath C *et al.* 2021. Suberin plasticity to developmental and exogenous cues is regulated by a set of MYB transcription factors. *Proceedings of the National Academy of Sciences, USA* **118**: e2101730118.

Sijmons PC, Kolattukudy PE, Bienfait FH. 1985. Iron deficiency decreases suberization in bean roots through a decrease in suberin-specific peroxidase activity. *Plant Physiology* **78**: 115–120.

Soliday CL, Kolattukudy PE, Davis RW. 1979. Chemical and ultrastructural evidence that waxes associated with the suberin polymer constitute the major diffusion barrier to water vapor in potato tuber (*Solanum tuberosum* L.). *Planta* **146**: 607–614.

Soukup A, Tylová E. 2018. Apoplastic barriers: their structure and function from a historical perspective. In: Sahi VP, Baluška F, eds. *Concepts in cell biology –*

history and evolution. Cham, Switzerland: Springer International Publishing, 155–183.

Steudle E, Meshcheryakov AB. 1996. Hydraulic and osmotic properties of oak roots. *Journal of Experimental Botany* **47**: 387–401.

Steudle E, Murrmann M, Peterson CA. 1993. Transport of water and solutes across maize roots modified by puncturing the endodermis (further evidence for the composite transport model of the root). *Plant Physiology* **103**: 335–349.

Steudle E, Oren R, Schulze ED. 1987. Water transport in maize roots: measurement of hydraulic conductivity, solute permeability, and of reflection coefficients of excised roots using the root pressure probe. *Plant Physiology* **84**: 1220–1232.

Steudle E, Peterson CA. 1998. How does water get through roots? *Journal of Experimental Botany* **49**: 775–788.

Stoláriková M, Vaculík M, Lux A, Baccio D, Minnocci A, Andreucci A, Sebastiani L. 2012. Anatomical differences of poplar (*Populus* × *euramericana* clone I-214) roots exposed to zinc excess. *Biologia* **67**: 483–489.

Su Y, Feng T, Liu C-B, Huang H, Wang Y-L, Fu X, Han M-L, Zhang X, Huang X, Wu J-C *et al.* 2023. The evolutionary innovation of root suberin lamellae contributed to the rise of seed plants. *Nature Plants* **9**: 1968–1977.

Suresh K, Zeisler-Diehl VV, Wojciechowski T, Schreiber L. 2022. Comparing anatomy, chemical composition, and water permeability of suberized organs in five plant species: wax makes the difference. *Planta* **256**: 1–13.

Taiz L, Zeiger E. 2002. *Plant physiology*. Sunderland, MA, USA: Sinauer Associates.

Tuskan GA, Difazio S, Jansson S, Bohlmann J, Grigoriev I, Hellsten U, Putnam N, Ralph S, Rombauts S, Salamov A. 2006. The genome of black cottonwood, *Populus trichocarpa* (Torr. & Gray). *Science* **313**: 1596–1604.

Ursache R, De Jesus Vieira Teixeira C, Dénervaud Tendon V, Gully K, De Bellis D, Schmid-Siegert E, Grube Andersen T, Shekhar V, Calderon S, Pradervand S *et al.* 2021. GDSL-domain proteins have key roles in suberin polymerization and degradation. *Nature Plants* **7**: 353–364.

Vishwanath SJ, Delude C, Domergue F, Rowland O. 2015. Suberin: biosynthesis, regulation, and polymer assembly of a protective extracellular barrier. *Plant Cell Reports* **34**: 573–586.

Wang P, Calvo-Polanco M, Reyt G, Barberon M, Champeyroux C, Santoni V, Maurel C, Franke RB, Ljung K, Novak O *et al.* 2019. Surveillance of cell wall diffusion barrier integrity modulates water and solute transport in plants. *Scientific Reports* **9**: 4227.

Zimmermann HM, Hartmann K-D, Schreiber L, Steudle E. 2000. Chemical composition of apoplastic transport barriers in relation to radial hydraulic conductivity of corn roots (*Zea mays* L.). *Planta* **210**: 302–311.

Supporting Information

Additional Supporting Information may be found online in the Supporting Information section at the end of the article.

Fig. S1 Relationship and amino acid sequence of the targeted genes.

Fig. S2 Analytical and molecular screening results.

Fig. S3 Additional analytics data of 5-wk-long hydroponics focusing aliphatic compounds.

Fig. S4 Additional analytics data of 5-wk-long hydroponics focusing aromatic compounds.

Fig. S5 Reverse transcription quantitative polymerase chain reaction confirmation of outstanding RNA-sequencing genes.

Fig. S6 Additional analytics data of 7-wk-long hydroponics.

Fig. S7 Correlation of root water transport to suberin amount of root Zone B.

Table S1 Differential root expression analysis with focus on the genes targeted in the CRISP/Cas9 double-knock-out approach.

Table S2 *CYP86* family and CYP suberin biosynthesis genes.

Methods S1 More detailed Materials and Methods.

Notes S1 Vector Map.

Notes S2 Primer lists and results of the target gene sequencing.

Notes S3 Results of the RNA-sequencing analysis.

Please note: Wiley is not responsible for the content or functionality of any Supporting Information supplied by the authors. Any queries (other than missing material) should be directed to the *New Phytologist* Central Office.